**DEUTSCHES ELEKTRONEN – SYNCHROTRON**

DESY 92–060
April 1992


# Radiation Hardness of Silicon Detectors for Future Colliders

E. Fretwurst, N. Claussen, N. Croitoru, G. Lindström,
B. Papendick, U. Pein, H. Schatz, T. Schulz, R. Wunstorf

*I. Institut für Experimentalphysik, Universität Hamburg*

ISSN 0418-9833

**NOTKESTRASSE 85 · D-2000 HAMBURG 52**

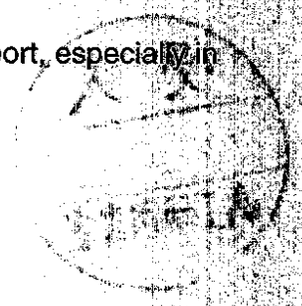

To be sure that your preprints are promptly included in the HIGH ENERGY PHYSICS INDEX, send them to (if possible by air mail):

| | |
|---|---|
| **DESY**<br>**Bibliothek**<br>**Notkestraße 85**<br>**W-2000 Hamburg 52**<br>**Germany** | **DESY-IfH**<br>**Bibliothek**<br>**Platanenallee 6**<br>**O-1615 Zeuthen**<br>**Germany** |

DESY 92-060
April 1992

ISSN 0418-9833

Sixth European Symposium on Semiconductor Detectors
Milano, February 24 - 26, 1992

# Radiation Hardness of Silicon Detectors for Future Colliders *

E. Fretwurst, N. Claussen, N. Croitoru†, G. Lindström, B. Papendick, U. Pein, H. Schatz, T. Schulz and R. Wunstorf

I. Institut für Experimentalphysik, Universität Hamburg, Germany

**Abstract**

The radiation hardness of silicon pad detectors, especially developed for the PLUG-Calorimeter of the H1 Experiment at HERA was investigated with respect to neutron and electron irradiation. Be(d,n)–neutrons with an average energy of $6.2MeV$ up to a fluence of $10^{15}n/cm^2$ and $1.8MeV$ electrons up to a dose of $1MGy$ ( $10^{16}e/cm^2$ ) were used. Degradation effects of the diode properties regarding the reverse current, depletion voltage and charge collection efficiency are studied at room temperature and with no bias applied during irradiation. Special emphasis is put on the separation of the respective damage generation and its subsequent self annealing. The observed effects are discussed with respect to radiation levels to be envisioned for experiments with future colliding beam machines.

## 1 Introduction

The very intense radiation fields connected with the high luminosity of future colliding beam machines (LHC, SSC) make radiation hardness a most urgent demand for all detector components. As an example for a LHC luminosity of $10^{34}cm^{-2}s^{-1}$ an annual neutron fluence of up to $10^{14}n/cm^2$ has been estimated in the forward region of a realistic detector configuration [1]. For the same pseudorapidity $\eta \simeq 2.5$ the charged particle dose, dominated mainly by the electromagnetic component, is in the order of $10kGy$ per year.

Radiation induced damage effects in silicon detectors can be roughly divided into two separate components. The dominant part is due to the bulk damage induced by the non-ionizing energy loss of the bombarding particles. In this respect neutron irradiation is much more effective leading to a much higher mean energy transfer to the primary knock on atom (PKA) than that by electrons. This is illustrated in fig.1 showing the non-ionizing energy loss (right scale) respectively the displacement damage cross section (left scale) as function of energy [2][3] . For example the ratio of the damage cross section for $1.8MeV$ electrons to that of $1MeV$ neutrons is about $10^{-2}$ .

In the following sections we describe results of our ongoing systematic investigations of radiation damage effects [4] - [8] . Degradation of the detector properties regarding the reverse current, depletion voltage, charge collection efficiency and surface effects are studied at room temperature. Special emphasis is put on the separation of the respective damage generation and its subsequent self annealing. Only in this way it is possible to calculate the resulting effect during long term exposures under realistic operation conditions at future colliders [9][10] . Additional investigations referring also to damage effects at $-20degrC$ and subsequent annealing at room temperature are included in the SITP report given at this conference [10] .

*work supported in part by BMFT under contract 05 5HH19 I
†on leave of absance from Tel Aviv University, Israel



## 2 Experimental Technique

Numerous irradiation experiments were performed mainly with $6.2MeV$ neutrons ( from the Be(d,n) reaction ) and $1.8MeV$ electrons. The parameters of the different radiation fields are listed in table 1. High neutron intensities of $10^{10}n/cm^2s$ could be achieved by the Be(d,n)–source at a distance of $10cm$ from the target. All measurements and calculations with respect to the neutron dosimetry were carried out by Brede et al. [11] . Details of the experimental set-up and dosimetry for electron irradiations can be found in [12] . All particle fluences were normalized to equivalent values for $1MeV$ neutrons. In this way the trivial dependence of the observed damage on the non-ionizing energy loss of different particles and energies is taken into account. For each radiation a corresponding hardness parameter $\kappa$ was derived in such a way that $\Phi(E_n = 1MeV) = \kappa \cdot \Phi(E)$ , where $\Phi(E)$ is the normal fluence for a given particle type and energy and $\Phi(E_n = 1MeV)$ is the equivalent $1MeV$ neutron fluence leading to the same non-ionizing energy loss. The $\kappa$ -values for neutrons were calculated using the damage cross sections of ref. [2] and for the case of electrons we used the non-ionizing energy loss from ref. [3] (see table 1).

The silicon detectors used in our investigations are mainly of the planar-surface barrier type. They were fabricated in our own laboratory from high resistivity ( $6k\Omega cm$ ) n-type material (Wacker-Chemitronics) with a thickness of $400\mu m$ . Different geometries of rectifying contacts with areas between 0.2 and $2cm^2$ were used in order to study possible edge effects. As outlined in a previous paper [8] the front electrode (Au) overlapps the $SiO_2$ edge protection layer, forming a narrow field plate which acts like a MOS-capacitor connected in parallel to the diode junction.

## 3 Change of Effective Impurity Concentration

The change of the effective impurity concentration due to radiation induced defects is derived from the depletion voltage via $C-V$ measurements. As long as moderate neutron fluences are concerned the measured $C-V$ characteristics are frequency independent indicating that the change of the depletion voltage is dominated by a corresponding change of the shallow dopant concentration only (dopant removal ). After irradiation with high fluences ( $\Phi > 10^{13}n/cm^2$ ) a strong frequency dependence of the $C-V$ curves is observed [8] in agreement with results reported by Kraner and Li [13][14] . In ref.

[14] this effect is discussed in detail. In their model the depletion voltage is not only determined by shallow dopants but also by deep defect centers. The charge state of these centers depends on the position of the defect energy level with respect to the Fermi level in the band gap. The junction capacitance in the low frequency limit and at bias voltages larger than several volts can be approximated by:

$$C(V, LF) = \frac{\epsilon_{Si} \cdot \epsilon_0}{\sqrt{\frac{2\epsilon_{Si} \cdot \epsilon_0}{q_0 \cdot N_{eff}} \cdot V}} \quad (1)$$

$N_{eff} = |N_d - N_t|$ is the compensated effective dopant concentration with $N_d = N_D - N_A$ , $N_D$ , $N_A$ being the donor and acceptor density respectively and $N_t$ is the concentration of the compensating deep trap level. It has been shown for many cases that the depletion voltage extracted from $C - V$ characteristics is identical to that resulting from charge collection measurements performed with short ranged alpha particles [7][8] .

In fig.2 the absolute value of $N_{eff}$ is plotted as function of the $1MeV$ equivalent neutron fluence. For comparison we include the much smaller effect resulting from electron irradiation. The neutron data show a conduction type inversion at about $2 \cdot 10^{12} n/cm^2$ and a linear increase of an acceptor like defect concentration above $10^{13} n/cm^2$ (see [5] – [8][15] ). As discussed in a previous paper [8] the experimental results for neutron irradiation are corrected for all self annealing effects including those during and in between successive exposures. The used annealing function (eq.(1) of ref. [8] is demonstrated in fig.3 together with measured values obtained for $\Phi < 5 \cdot 10^{12} n/cm^2$ . Our older results have now been extended to much larger annealing times up to 1 year, this way enabling us to derive the necessary predictions for real operational conditions in prospective LHC or SSC experiments [10] . A reanalysis of these data results in slightly changed parameters for the longest time constants. They are listed in table 2 (compare with table 2 of ref. [8]).

In modification of our previous empirical approach [8] we apply the following model for the fluence dependence of the effective dopant concentration. It is based on the fact that the annealing temperature of the vacancy-boron complex defect is only $170K$ [16] and therefore a possible boron removal does not play a significant role for room temperature irradiation. In contrast donor removal due to the formation of E-centers (vacancy-phosphorus complex) is quite likely; this defect anneals out at about $420K$ [17] . In addition we have to assume the creation of acceptor like deep defect centers as before [8] . This leads finally to the following formula:

$$N_{eff}(\Phi) = N_{D,0} \cdot exp(-c \cdot \Phi) - (N_{A,0} + b \cdot \Phi) \quad (2)$$

where $N_{D,0}$, $N_{A,0}$ are the donor resp. acceptor concentrations before irradiation. This ansatz was proven to be correct for neutron irradiation by analyzing data derived at low and medium fluences for different detectors together with data of one detector irradiated up to $10^{14} n/cm^2$ . We chose only detectors with approximately the same initial effective donor concentration $N_{D,0} - N_{A,0}$ within a limit of 5 % . Furthermore we supposed that the difference in the boron concentration of the individual detectors can be neglected. An estimate for $N_{A,0}$ was achieved by an extrapolation of $N_{eff}(\Phi)$ values for fluences above $10^{13} n/cm^2$ to $\Phi = 0$ (see eq.(2)). This results in a value of $N_{A,0} = 2.4 \cdot 10^{11} cm^{-3}$ . A comparison between the experimental data and a fit according to eq.(2) with parameters



$c = (3.5 \pm 0.2) \cdot 10^{-13} cm^2$ and $b_n = (0.079 \pm 0.006) cm^{-1}$ is shown in fig.4. The acceptor creation parameter $b_n$ is only slightly changed with respect to the previous publication [8] , whereas the parameter $c_n$ turns out to be lower by a factor of 2. It should be mentioned that the $b$ -values presented in [10] for n- and p-type material deviate from our value only by about 15%.

For electrons, using the same ansatz of eq.(2) and assuming the same boron concentration of $N_{A,0} = 2.4 \cdot 10^{11} cm^{-3}$ as obtained from the neutron irradiation data we get $c_e = (3.5 \pm 0.8) \cdot 10^{-15} cm^2$ and $b_e = 0$ . Although $c_e$ is extracted with respect to the equivalent $1MeV$ neutron fluence and therefore effects due to the different non-ionizing energy loss of electrons and neutrons are taken into account there is a very large remaining effect of $c_e / c_n \approx 10^{-2}$ . This discrepancy indicated strong differences of the defect formation by neutrons and electrons. One reason may be attributed to a high recombination rate of primary defects ( e.g. metastable closed pairs) induced by electrons. On the other hand the mean distance between the primary silicon interstitial and vacancy created by neutrons is much larger and hence a recombination is very unlikely [18].

It should be mentioned here that despite of the quite reassuring way of describing the effective dopant concentration as function of the neutron fluence we do not have a similarly consistant picture for the self annealing behaviour. In particular the reverse annealing at large time durations remains to be an open question.

# 4 Increase of Reverse Current

As reported in a previous paper [8] the $I - V$ characteristics at high neutron fluences above $10^{13} n/cm^2$ saturate at a lower voltage than necessary for total depletion. On the other hand the current saturation voltage and the depletion voltage are identical at low fluences. As we are confident that the $C - V$ measurements reflect the real reach through of the electric field (see section 3) we are now plotting the detector current at this value as function of neutron fluence (fig.5). Two fluence regions are obvious. Using the standard equation for the fluence dependence of the bulk current increase $\Delta I/V = \alpha \cdot \Phi$ we observe. a damage coefficient of $\alpha_n = 8 \cdot 10^{-17} A/cm$ for $\Phi_n < 8 \cdot 10^{12} n/cm^2$ . Above a transition region related to type inversion $\alpha_n$ increases by a factor of about 2.5. Such behaviour was also observed for irradiations at $-20 degrC$ and for detectors fabricated by different technologies (see [10]).

Again we include in fig.5 results for electron irradiation using the normalization of the electron fluence as given in section 3. Here we derive a damage coefficient $\alpha_e = 4.2 \cdot 10^{-18} A/cm$ and hence $\alpha_e / \alpha_n \approx 0.05$ ( $\alpha_n$ taken for low fluences). This ratio is therefore again much smaller than expected from the relative non-ionizing energy loss alone. Van Lint [19] reported corresponding damage ratios for $3MeV$ electrons (also with respect to $1MeV$ neutrons)in low resistivity n-type material (1 and 10 $\Omega cm$ ). Normalizing his data to $1.8MeV$ electrons and extrapolating them with respect to the material resistivity a ratio of about 0.03 would be derived in good agreement with our own result.

All data plotted in fig.5 are corrected for self annealing. The corresponding annealing functions are presented in fig. 6 for neutrons and electrons. The parameters of the applied formula (see ref. [8] ) are listed in table 3. For neutron irradiated samples we observe again a different behaviour for low and high fluences respectively. Well above type inversion (

$\Phi > 10^{13} n/cm^2$ ) the amplitudes of the two short time constants are considerably larger than the values for low fluences. In addition a constant term is observed in contrast to the non-inverted sample. These deviations may be due to surface effects concerning the change of the rectifying contact after inversion. The annealing effect for electron irradiated detectors is quite small compared to neutron irradiation. Only 40 % of the initial current anneals out over a period of about 1 year.

# 5 Degradation of Charge Collection Efficiency

Using short ranged monoenergetic alpha particles incident on the front and rear electrode of the detector it is possible to measure the charge collection efficiency resulting from the electron resp. hole contribution separately [5]. Measurements are performed as function of bias voltage above total depletion. Using the known drift velocities as function of electric field [20] we were able to extract the relevant trapping time constants for electrons and holes. These values are plotted as function of neutron fluence in fig.7. For a given trap we expect $N_t \propto \Phi$ . As $\tau \propto 1/N_t$ we would get a linear dependence of $1/\tau$ as function of $\Phi$ . For holes this expectation is confirmed in the full fluence range up to $2 \cdot 10^{13} n/cm^2$ . However for electrons a significant deviation from the initial slope is observed at $1 \cdot 10^{13} n/cm^2$ . These measurements could not be carried out immediately after irradiation; appreciable self annealing prior to the measurements could therefore not be avoided. Hence the onset of the increased electron trapping may very well be connected with type inversion to be expected at $2 \cdot 10^{12} n/cm^2$ immediately after irradiation and probably delayed here according to annealing [5] . Again this point needs further investigation. From fig.7 we get:

$$1/\tau = \gamma \cdot \Phi \tag{3}$$

with $\gamma_h = 2.7 \cdot 10^7 cm^2/s$ and $\gamma_e = 1.2 \cdot 10^{-6} cm^2/s$ for $\Phi > 10^{13} n/cm^2$ . A detailed investigation with respect to the change of the internal electric field profile and trapping phenomena in neutron damaged detectors using the method of current pulse shape measurements is presented in the paper of Kraner et al. [21] at this conference. It is reassuring that both methods lead to approximately the same results.

From our $\tau$ -values we can deduce the resulting change in the charge collection for minimum ionizing particles. If we suppose e.g. an irradiation of $5 \cdot 10^{13} n/cm^2$ during a total exposure time of $10^7 s$ (1 equivalent operational year) leading to a depletion voltage of about $130V$ for a $400\mu m$ thick detector and if a bias voltage of $200V$ is applied we get a charge collection deficiency of $\Delta Q/Q_0 = 12\%$ for mip's. This is in very nice agreement with recent results reported by Lemeilleur et al. [15] .

# 6 Surface Effects

On top of the described bulk effects surface damage in the oxide passivation layers may be expected from ionizing radiation. Examples of such effects have been measured following electron irradiation and are shown in figs.8-11. As discussed in detail in a previous paper the $I-V$ characteristic of our detectors is strongly influenced by the field plate overlapping



the oxide edge [4] . At the onset of depletion underneath the field plate at about flat band voltage the $SiO_2 - Si$ interface states become active for carrier generation which is easily seen in a steep increase of the detector current. This effect is shown in fig.8 for a detector irradiated with an electron dose of $96kGy$. Using the voltage dependence of the bulk generation current ( $I \propto \sqrt{V}$ ) we are able to extract the surface contribution only. This can be represented by the corresponding surface generation velocity:

$$S_0 = I_S / A_S \cdot q_0 \cdot n_i \tag{4}$$

where $I_S$ is the surface current related to the interface states, $A_S$ the field plate area and $n_i$ the intrinsic carrier density. We obtain an overall linear dependence as function of the electron dose (see fig.9). This is in contrast to results of Snow et al. [22] which show a saturation above $0.1 MGy$ . The deviation may be due to a dose dependent lateral extension of the electric field beyond the geometrical limit of the field plate in our case. Therefore, according to an increase of $A_S$ with fluence more interface states can contribute to the surface current.

Another well known effect is the change of the flat band voltage originating from radiation induced trapped oxide charges and interface states (see e.g. [23] ). As an example in fig.10 the change of the $C-V$ characteristic at low bias voltages with increasing electron dose is demonstrated. From the shift of the MOS related capacitance curves we deduced the change of the flat band voltage as function of electron dose (fig.11). The measured values can be best represented by $\Delta V_B \propto D^{0.4}$ ( $D$ being the absorbed dose). Such behaviour cannot be interpreted in a simple way as the trapped oxide charge as well as the charge of radiation induced interface traps depend in a complicated way on the transport phenomena of the created electron hole pairs in the oxide, the technology of the oxide growth and on further conditions during irradiation (see e.g. [23] ).

# 7 Conclusions

Our ongoing systematic studies of the radiation hardness of silicon detectors have been further complemented by a comparison of neutron and electron induced damage effects up to a fluence of $10^{15} n/cm^2$ resp. a dose of $1 MGy$ . The results may be summarized as follows:

- The dependence of the effective dopant concentration as function of particle fluence can be well represented by a simple model taking donor removal and a fluence proportional creation of acceptor like states into account. Parameters for an appropriate function are derived. A neutron irradiation by $10^{14} n/cm^2$ during an extended period of time, allowing for self annealing, would e.g. lead to a depletion voltage of only $140V$ for $250\mu m$ thick detectors. The donor removal due to electron irradiation is lower by a factor of 100 even if normalized to the same non-ionizing energy loss. No acceptor creation is observed in this case.

- The bulk current increase is linear with respect to the particle fluence for both neutron and electron irradiation. The value of $\alpha_n = 8 \cdot 10^{-17} A cm^{-1}$ for neutrons is confirmed for fluences up to $10^{13} n/cm^2$ . The electron effect, normalized as above,

is smaller by a factor of 20. Possibly due to surface effects the neutron related value $\alpha_n$ increases above type inversion by a factor of 2.5. After considerable self annealing this discrepancy is however strongly reduced again. It will therefore not play a significant role for real operational conditions.

- Parameters for the charge collection efficiency have also been derived separately for the electron and hole contribution following neutron irradiations up to $2 \cdot 10^{13} n/cm^2$. Extrapolating these data to $10^{14} n/cm^2$ we expect a signal pulse height degradation for mip's of less than 20% for $250 \mu m$ thick detectors biased at $200V$.. Within the investigated electron fluence range no appreciable pulse degradation could be observed.

- Surface effects induced by electrons and attributed to the $SiO_2$ passivation layer as well as the $SiO_2 - Si$ interface are clearly visible and have been studied up to $1 MGy$ $(100 Mrad)$ . Even at this extremely high dose the observed effects are tolerable for safe detector operation. However an appreciable change may be expected if the detectors are irradiated under bias.

- Self annealing at room temperature has been studied in more detail up to 1 year after irradiation enabling us to predict the detector performance under real operational conditions. Although the self annealing functions for both the effective dopant concentration and the current increase can be well parametrized using a set of exponentials with different time constants and amplitudes no physical model for understanding the relevant effects can be presented so far.

## Acknowledgements

Special thanks are due to the staff of the irradiation facility at the Physikalisch-Technische-Bundesanstalt Braunschweig, the Universitäts-Krankenhaus Eppendorf, Hamburg and the Telefunken-System-Technik at Wedel/Hamburg. We greatly appreciate extensive discussions with H. W. Kraner and Z. Li (BNL) as well as J. Walter (IntraSpec, Oak Ridge).



## References

[1] A. Ferrari, P.R. Sale, A. Fasso and G.R. Stevenson, EAGLE Internal Note, CAL-NO-005, Nov. 1991

[2] M.S. Lazo, D.M. Woodall and P.J. McDaniel, Sandia Nat. Lab., Techn. Report SAND87 - 0098, Vol.1, 1987

[3] A. Van Ginneken, Fermi Nat. Acc. Lab., Report FN - 522, Oct. 1989

[4] E. Fretwurst, H. Herdan, G. Lindström, U. Pein, M. Rollwagen, H. Schatz, P. Thomsen and R. Wunstorf, Nucl. Instr. and Meth. in Phys. Res. A 288 (1990) 1

[5] G. Lindström, M. Eberle, I. Fedder, E. Fretwurst, U. Pein, V. Riech, H. Schatz, R. Wunstorf, C. Zeitnitz, N. Croitoru, R. Darvas, A. Seidman, R. Böttger and H. Schölermann in: 5th International Conference on Instrumentation for Colliding Beam Physics, Inst. of Nucl. Phys., Novosibirsk 1990, Ed. E.P. Solodov (World Scientific, Singapore, 1990) p. 331 and DESY Report, DESY 90-109, Sept. 1990

[6] G. Lindström, M. Benkert, E. Fretwurst, T. Schulz, and R. Wunstorf in: International Conference on Calorimetry in High Energy Physics, Fermilab, Batavia 1990, Eds. D.F. Andersen, M. Derrick, H. E. Fisk, A. Para and C. M. Sazana (World Scientific, Singapore, 1991) p. 467

[7] R. Wunstorf, M. Benkert, E. Fretwurst, G. Lindström, T. Schulz, N. Croitoru, R. Darvas, M. Mudrik, R. Böttger and H. Schölermann, Nucl. Phys. B (Proc. Suppl.) 23A (1991) 324

[8] R. Wunstorf, M. Benkert, N. Claussen, N. Croitoru, E. Fretwurst, G. Lindström and T. Schulz, Nucl. Instr. and Meth. in Phys. Res. 1992, in print

[9] G. Lindström, SITP internal report, SITP-TR-002, 1991, p. 1-11

[10] SITP - Collaboration, Sixth European Symposium on Semiconductor Detectors, Milano, Febr. 1992, this Volume

[11] H.J. Brede, G. Dietze, K. Kodo, U.J. Schrewe, F. Tancu and C. Wen, Nucl. Instr. and Meth. in Phys. Res. A274 (1989) 332 and H.J. Brede, private communication

[12] T. Schulz, diploma thesis, University of Hamburg, 1991

[13] Z. Li and H.W. Kraner, IEEE Trans. Nucl. Sci. NS-38, No.2 (1991 244

[14] Z. Li, W. Chen and H.W. Kraner, Nucl. Instr. and Meth. in Phys. Res. A308 (1991) 585

[15] F. Lemeilleur, M. Glaser, E.H.M. Heijne, P. Jarron and E. Occelli, Nuclear Science Symposium, Santa Fe, Nov. 1991, in print

[16] G.D. Watkins, in: Deep Centers in Semiconductors, Ed. S.T. Pantelides (Gordon and Breach, New York, 1986) p. 167

[17] L.C. Kimerling, H.M. DeAngelis and C.P. Carnes, Phys. Rev. B3 (1971) 427

[18] G.P. Mueller and C.S. Guenzer, IEEE Trans. Nucl. sci. NS-27, No.6 (1980)1474 and G.P. Mueller, N.D. Wilsey and M. Rosen, IEEE Trans. Nucl. Sci. NS-29, No.6 (1982) 1493

[19] V.A.J. van Lint, T.M. Flanagan, R.E. Leadon, J.A. Naber and V.C. Rogers, Mechanisms of Radiation Effects in Electronic Materials, Vol.1 (John Wiley & Sons, New York, 1980)

[20] C. Canalli and G. Ottaviani, J. Phys. Chem. Solids 32 (1971) 1707

[21] H.W. Kraner, E. Fretwurst and Z. Li, Sixth European Symposium on Semiconductor Detectors, Milano, Febr. 1992, this volume

[22] E.H. Snow, A.S. Grove and D.J. Fitzgerald, Proc. IEEE Vol.55 (1967) 764

[23] J.R. Srour and M. McGarrity, Proc. IEEE Vol.76, No.11 (1988) 1443



**Table 1: Parameters of the irradiation experiments**

| Radiation Type | E $[MeV]$ | Hardness Parameter $\kappa$ | Flux/Dose-Rate $[cm^{-2}s^{-1}]$ $/(Gys^{-1})$ | Fluence/Dose $[cm^{-2}]$ $/(Gy)$ | Fluence/Dose Error |
|---|---|---|---|---|---|
| neutrons | | | | | |
| T(p,n)$^3$He[1)] | 1.2 | 0.88 | $7 \cdot 10^6 - 1 \cdot 10^7$ | $7 \cdot 10^{10} - 1 \cdot 10^{12}$ | 4% |
| D(d,n)$^3$He[1)] | 5.0 | 1.69 | $1.5 \cdot 10^7$ | $4 \cdot 10^{11} - 2 \cdot 10^{12}$ | 3% |
| T(d,n)$^4$He[2)] | 14.1 | 1.88 | $1 \cdot 10^6 - 6 \cdot 10^8$ | $1 \cdot 10^9 - 3 \cdot 10^{12}$ | 5% |
| Be(d,n)B[1)] | 6.2 | 1.53 | $7 \cdot 10^8 - 1 \cdot 10^{10}$ | $2 \cdot 10^{10} - 8 \cdot 10^{14}$ | 5% |
| electrons[3)] | 1.8 | $1.07 \cdot 10^{-2}$ | $1 \cdot 10^{11} - 3 \cdot 10^{12}$ (28-843) | $1 \cdot 10^{12} - 6 \cdot 10^{15}$ $(3 \cdot 10^2 - 2 \cdot 10^6)$ | 2% |

[1)] Irradiation facilities at the Physikalisch-Technische Bundesanstalt, Braunschweig
[2)] Irradiation facility at the University Hospital, Hamburg
[3)] Irradiation facility at the Telefunken-System-Technik, Wedel

**Table 2: Time constants $\tau_i$ and relative amplitudes $A_i$ for $\Delta N_{eff}(t)/\Delta N_{eff}(0)$** (eq.(1) in ref.[8]) obtained from fitting the data given in fig.3:

| Time constants $\tau_i$ $[min]$ | Relative amplitudes $A_i$ |
|---|---|
| $(9.40 \pm 0.80) \cdot 10^0$ | $0.214 \pm 0.030$ |
| $(6.87 \pm 0.14) \cdot 10^1$ | $0.261 \pm 0.007$ |
| $(3.43 \pm 0.12) \cdot 10^2$ | $0.118 \pm 0.008$ |
| $(4.00 \pm 0.04) \cdot 10^3$ | $0.097 \pm 0.002$ |
| $(7.52 \pm 0.02) \cdot 10^4$ | $-0.107 \pm 0.001$ |
| $\infty$ | $0.417 \pm 0.004$ |

**Table 3: Time constants $\tau_i$ and relative amplitudes $A_i$ for annealing** of the bulk generation current obtained from fitting the data given in fig.6.

| Neutrons $\Phi = 6 \cdot 10^{11} n/cm^2$ | | Neutrons $\Phi = 2 \cdot 10^{13} n/cm^2$ | | Electrons $\Phi = 5 \cdot 10^{14}/cm^2$ | |
|---|---|---|---|---|---|
| Time constant $\tau_i$ $[min]$ | Relative amplitude $A_i$ | Time constant $\tau_i$ $[min]$ | Relative amplitude $A_i$ | Time constant $\tau_i$ $[min]$ | Relative amplitude $A_i$ |
| $1.78 \cdot 10^1$ | 0.16 | $1.29 \cdot 10^1$ | 0.20 | $6.2 \cdot 10^1$ | 0.25 |
| $1.19 \cdot 10^2$ | 0.11 | $8.54 \cdot 10^1$ | 0.30 | $5.5 \cdot 10^3$ | 0.10 |
| $1.09 \cdot 10^3$ | 0.13 | $1.83 \cdot 10^3$ | 0.13 | $7.0 \cdot 10^6$ | 0.65 |
| $1.47 \cdot 10^4$ | 0.20 | $9.50 \cdot 10^3$ | 0.13 | | |
| $6.70 \cdot 10^5$ | 0.40 | $\infty$ | 0.24 | | |

## Figure Captions:

**Fig.1:** Displacement damage cross section (left scale) resp. non-ionizing energy loss $NIEL$ (right scale) for neutrons [2] and electrons [3] as function of energy.

**Fig.2:** Absolute value of the effective dopant concentration versus normalized fluence for neutrons and electrons. The solid and dashed curves represent fits according to eq.(2).

**Fig.3:** Room temperature annealing data for the relative dopant concentration after neutron damage together with a fit (see text) and corresponding parameters given in table 2.

**Fig.4:** Fluence dependence of the effective dopant concentration. Solid curve: fit according to eq. (2); dashed lower and upper lines: acceptor creation resp. donor removal.

**Fig.5:** Increase of measured reverse current at total depletion as function of normalized particle fluence for $6.2MeV$ neutrons and $1.8MeV$ electrons.

**Fig.6:** Room temperature annealingof reverse current after $6.2MeV$ neutron (a) and $1.8MeV$ electron irradiation (b). The solid lines are fits to the data using parameters listed in table 3.

**Fig.7:** Dependence of $1/\tau$ for electrons and holes on the normalized $1MeV$ equivalent neutron fluence (see text).

**Fig.8:** Reverse current of an electron irradiated detector versus $V^{\frac{1}{2}}$ showing the oxide related surface contribution $I_S$ (see text).

**Fig.9:** Surface generation velocity $S_0$ (see eq.(4)) as function of absorbe electron dose. The solid line represents a mean slope of $0.017cm/sec/Gy$.

**Fig.10:** Capacitance-voltage characteristics after damage by different electron dose values demonstrating the shift of the flat band voltage.

**Fig.11:** Dependence of the flat band voltage shift on the electron radiation dose. The solid line corresponds to $\Delta V_{FB} \propto D^{0.4}$.



Fig.1

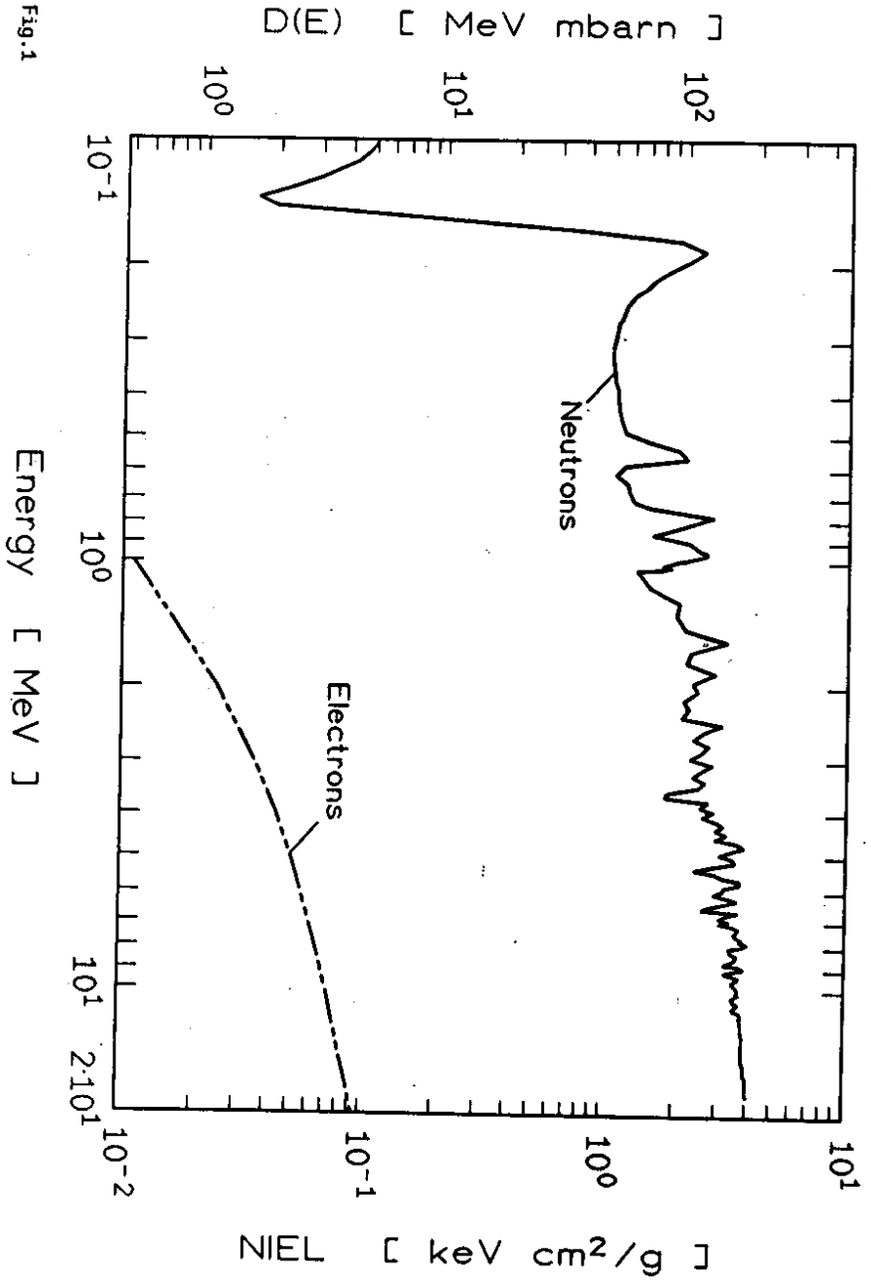

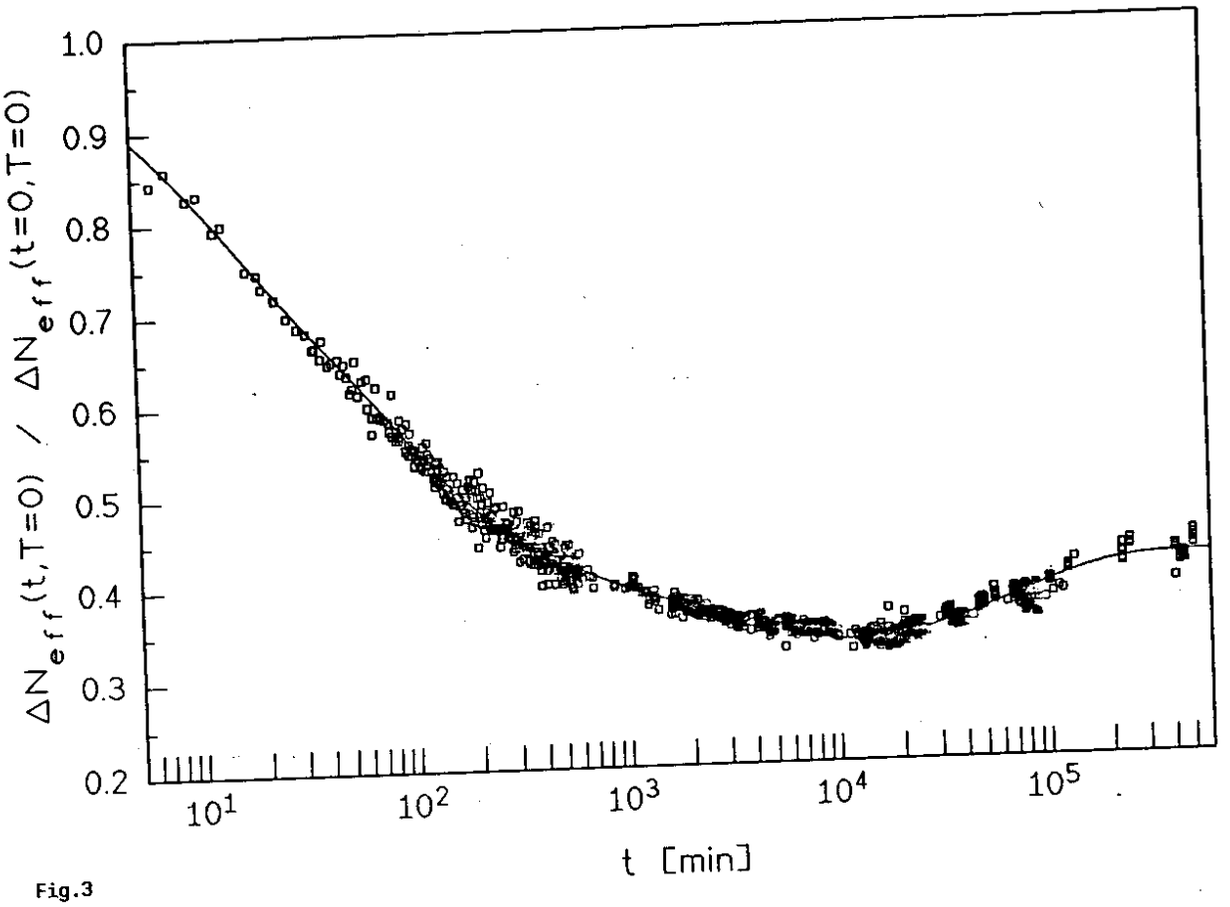
1.0
0.9
0.8
0.7
0.6
0.5
0.4
0.3
0.2
$\Delta N_{eff}(t,T=0) \;/\; \Delta N_{eff}(t=0,T=0)$
$10^1$
$10^2$
$10^3$
$10^4$
$10^5$
t [min]

Fig.3



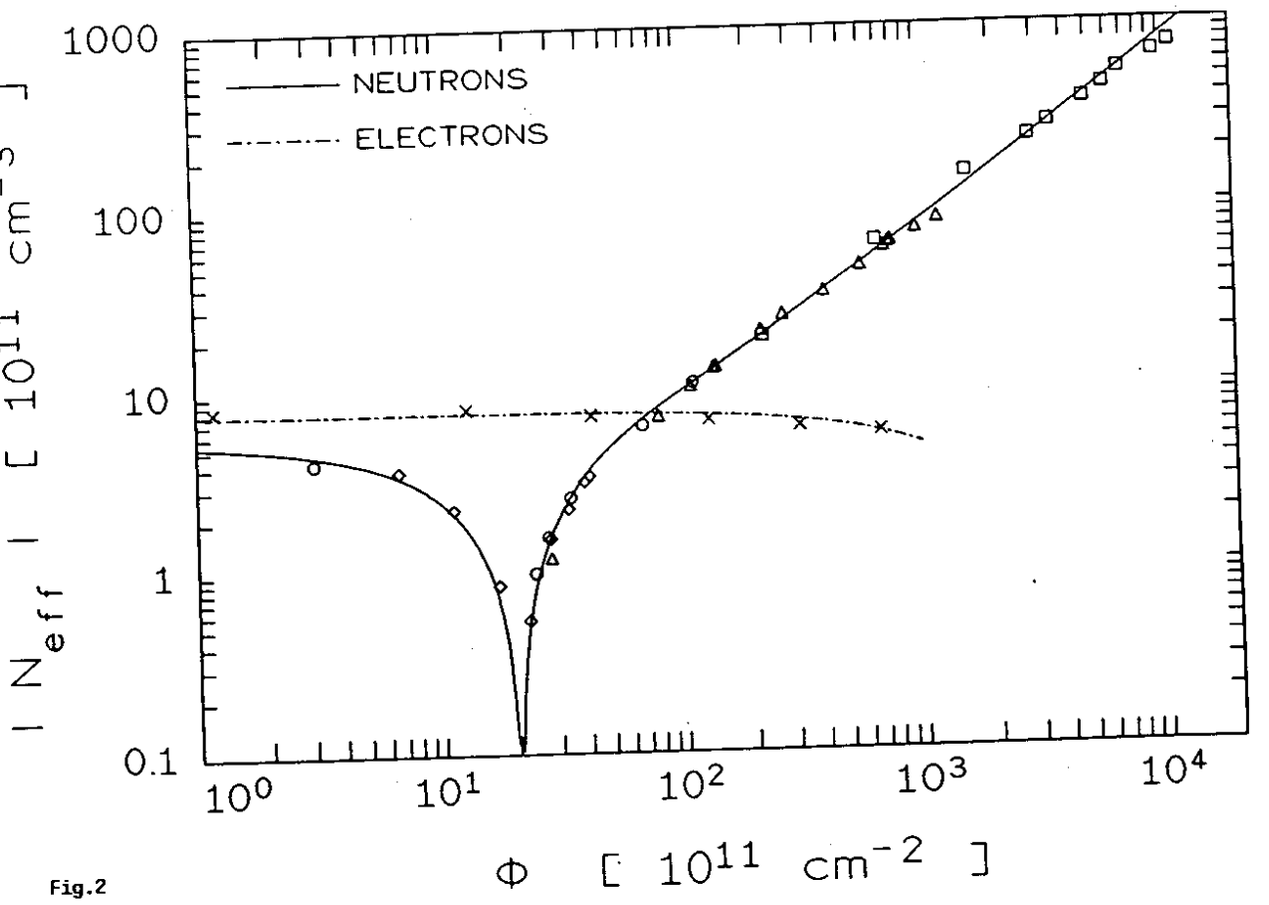
1000
100
10
1
0.1
NEUTRONS
ELECTRONS
$| N_{eff} |$ [ $10^{11}$ $cm^{-3}$ ]
$10^0$
$10^1$
$10^2$
$10^3$
$10^4$
$\Phi$ [ $10^{11}$ $cm^{-2}$ ]

Fig.2

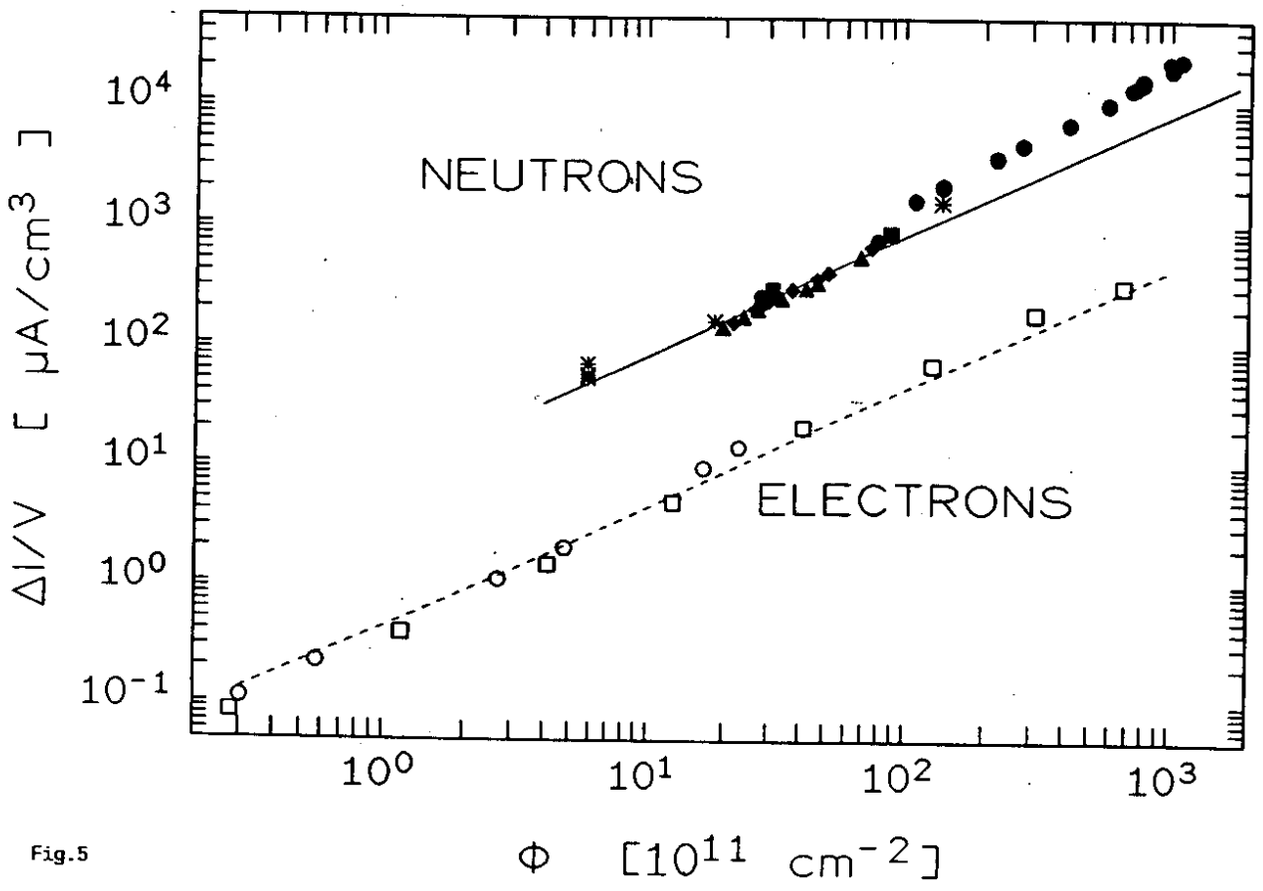
NEUTRONS
ELECTRONS
ΔI/V [ μA/cm³ ]
Φ [10¹¹ cm⁻²]

Fig.5



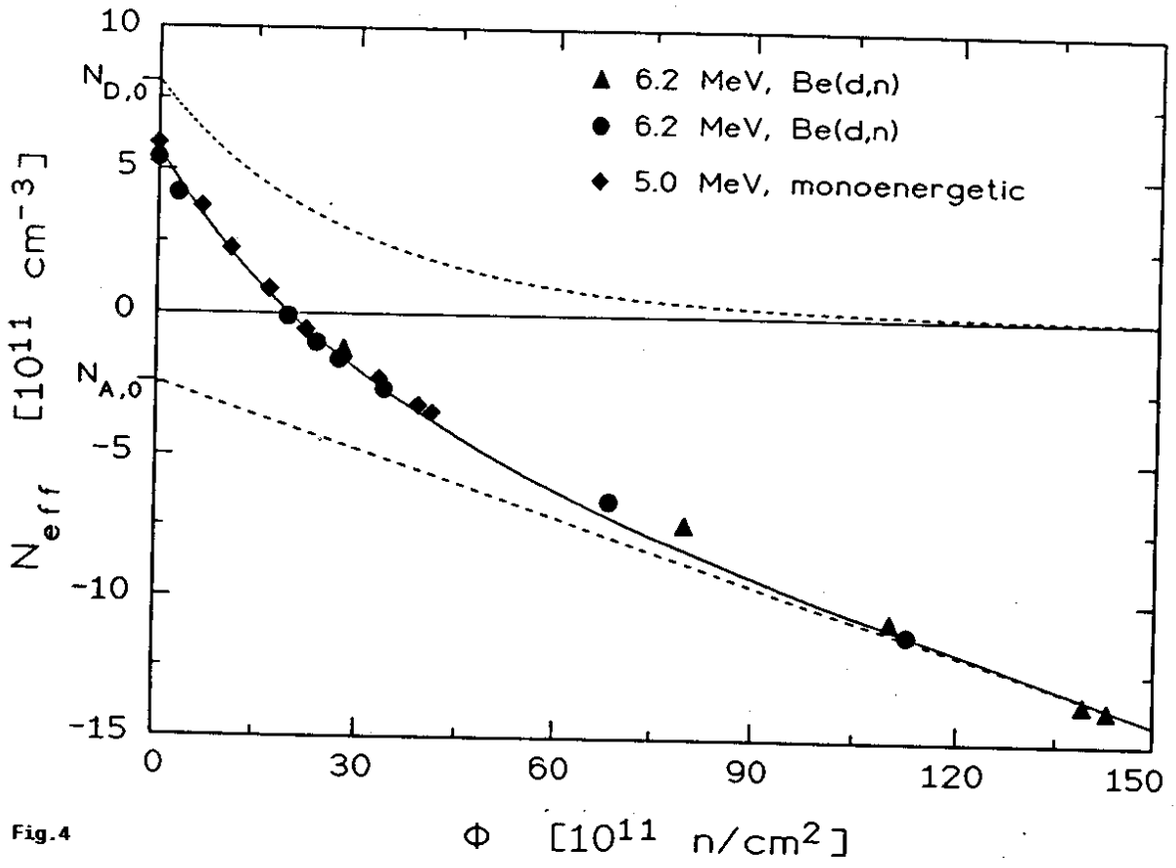
6.2 MeV, Be(d,n)
6.2 MeV, Be(d,n)
5.0 MeV, monoenergetic
N_D,0
N_A,0
N_eff [10¹¹ cm⁻³]
Φ [10¹¹ n/cm²]

Fig.4

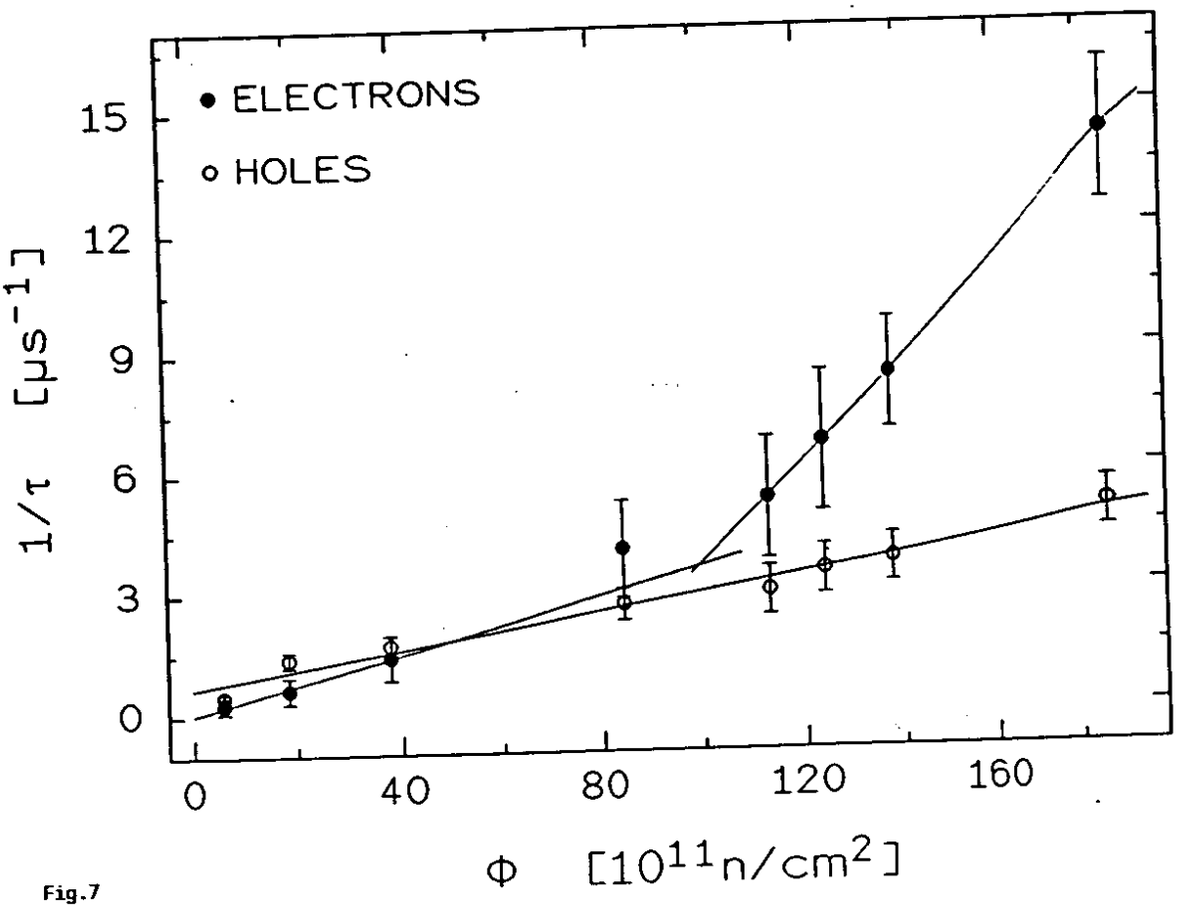
• ELECTRONS
o HOLES
1/τ [μs⁻¹]
Φ [10¹¹n/cm²]
0
3
6
9
12
15
0
40
80
120
160

Fig.7



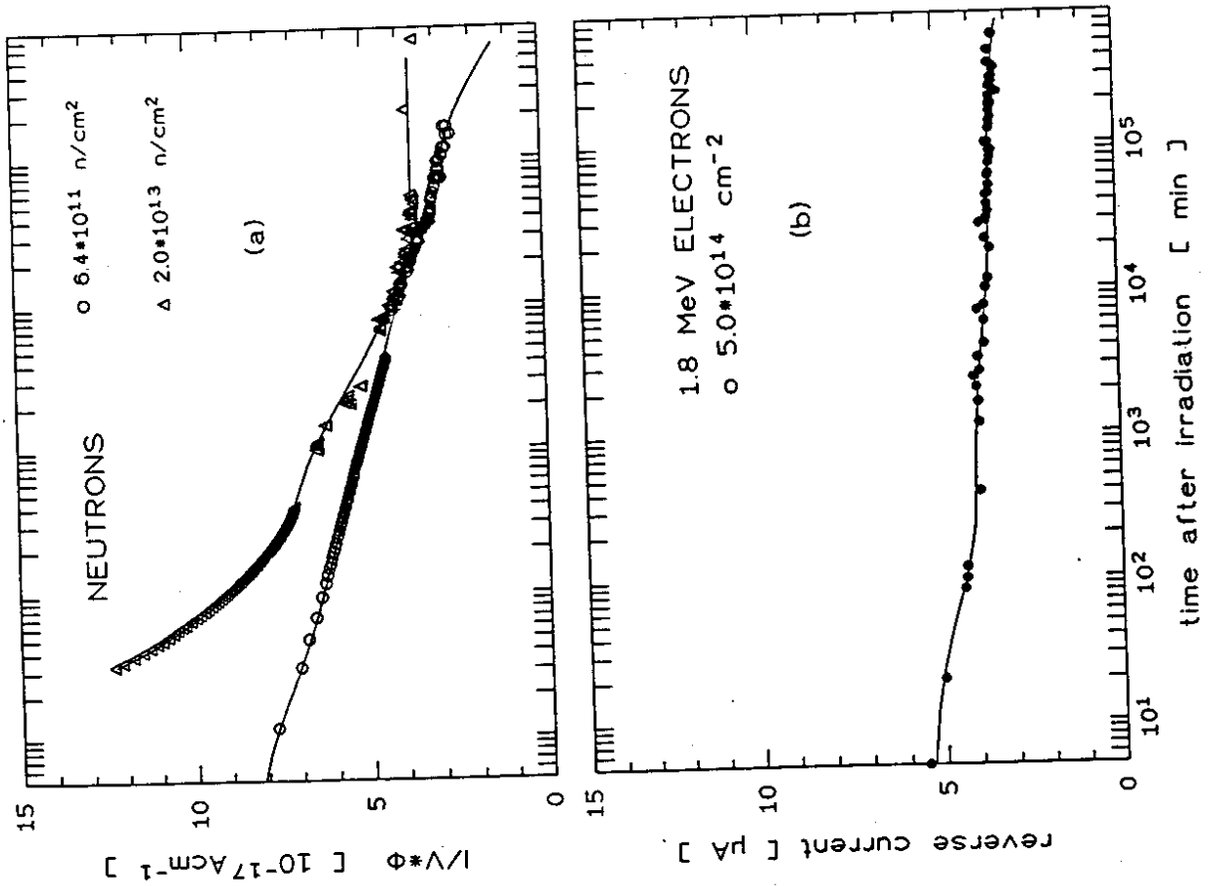
NEUTRONS
o 6.4*10¹¹ n/cm²
Δ 2.0*10¹³ n/cm²
(a)
1/V*Φ [ 10⁻¹⁷Acm⁻¹ ]
1.8 MeV ELECTRONS
o 5.0*10¹⁴ cm⁻²
(b)
reverse current [ μA ]
time after irradiation [ min ]

Fig.6

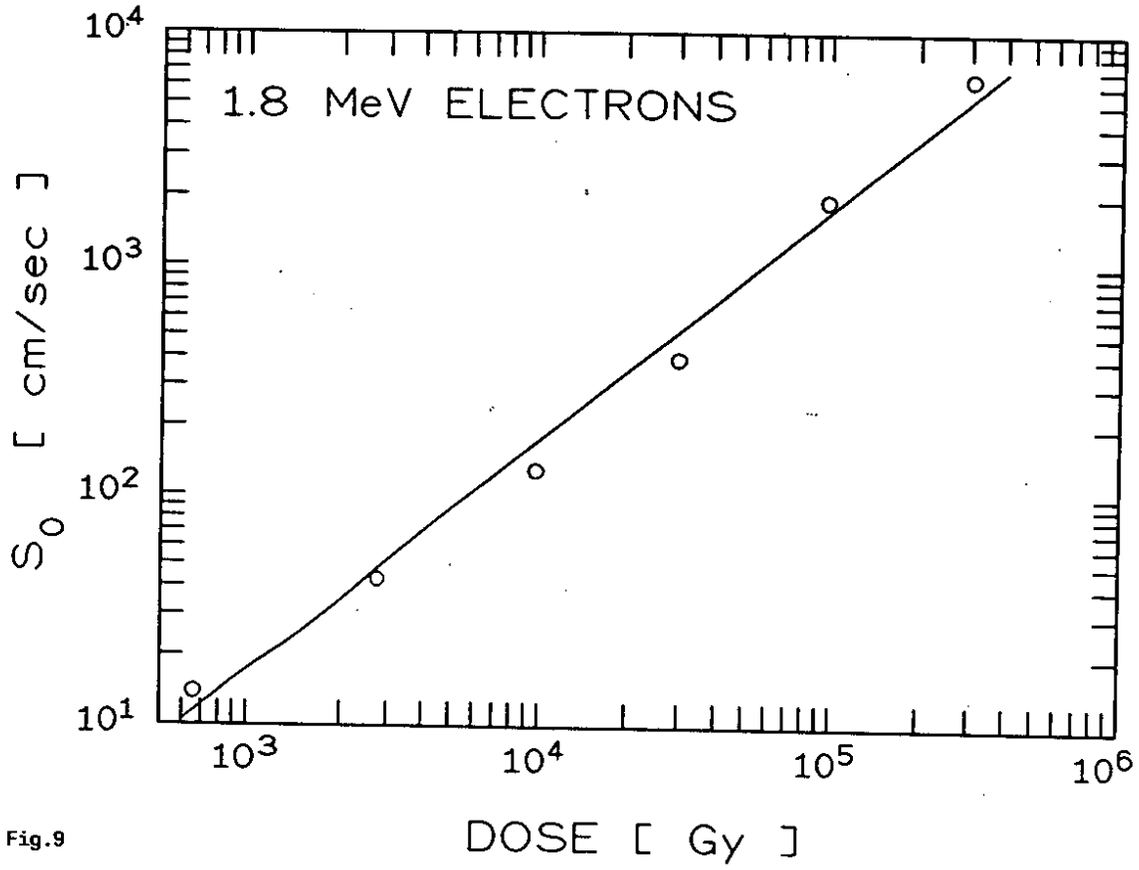
1.8 MeV ELECTRONS
$S_0$ [ cm/sec ]
$10^4$
$10^3$
$10^2$
$10^1$
$10^3$
$10^4$
$10^5$
$10^6$
DOSE [ Gy ]

Fig.9



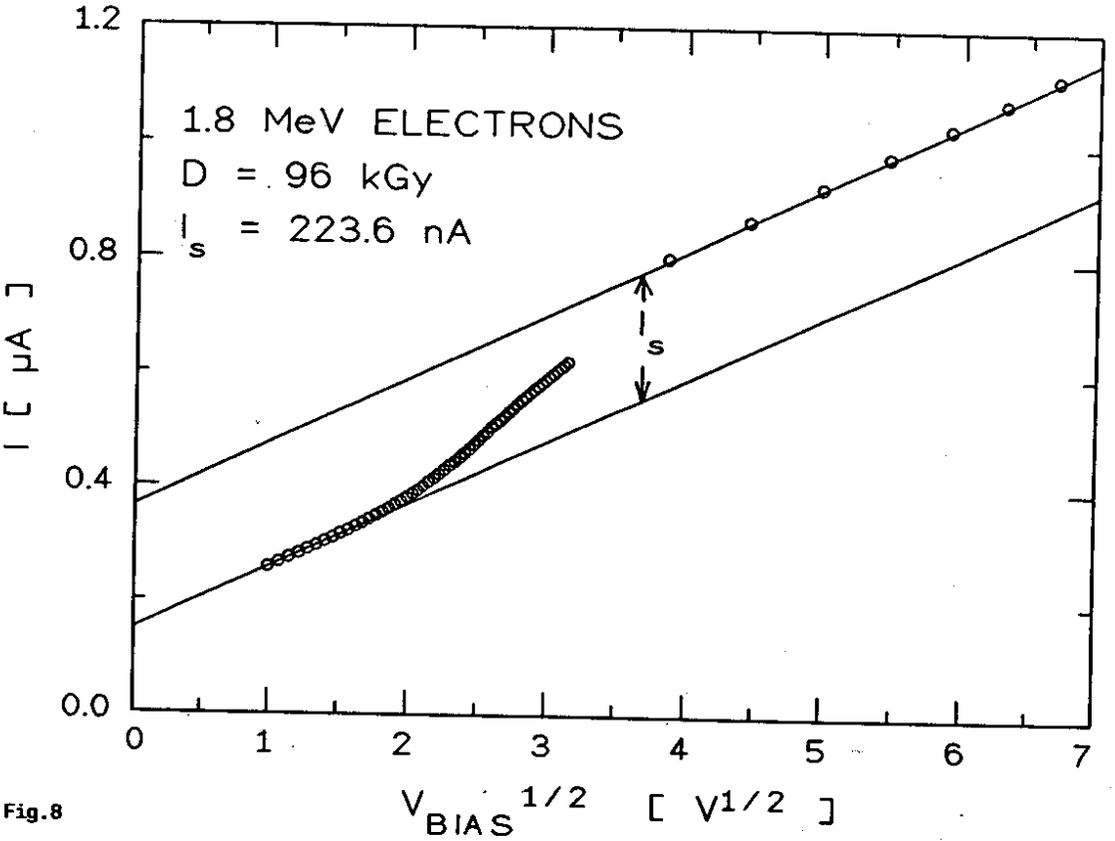
1.8 MeV ELECTRONS
D = 96 kGy
$I_s$ = 223.6 nA
$I_s$
I [ μA ]
1.2
0.8
0.4
0.0
0
1
2
3
4
5
6
7
$V_{BIAS}^{1/2}$ [ $V^{1/2}$ ]

Fig.8

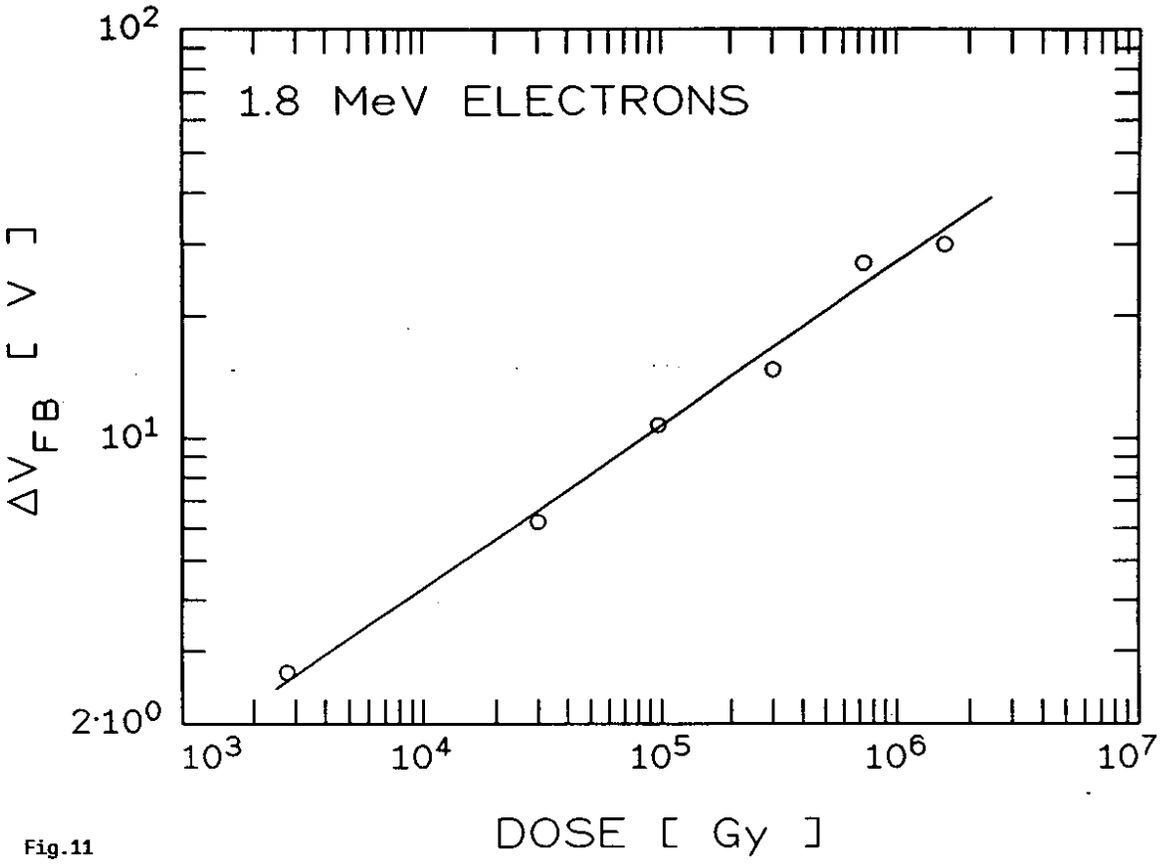
1.8 MeV ELECTRONS
$\Delta V_{FB}$ [ V ]
$10^2$
$10^1$
$2 \cdot 10^0$
$10^3$
$10^4$
$10^5$
$10^6$
$10^7$
DOSE [ Gy ]

Fig.11



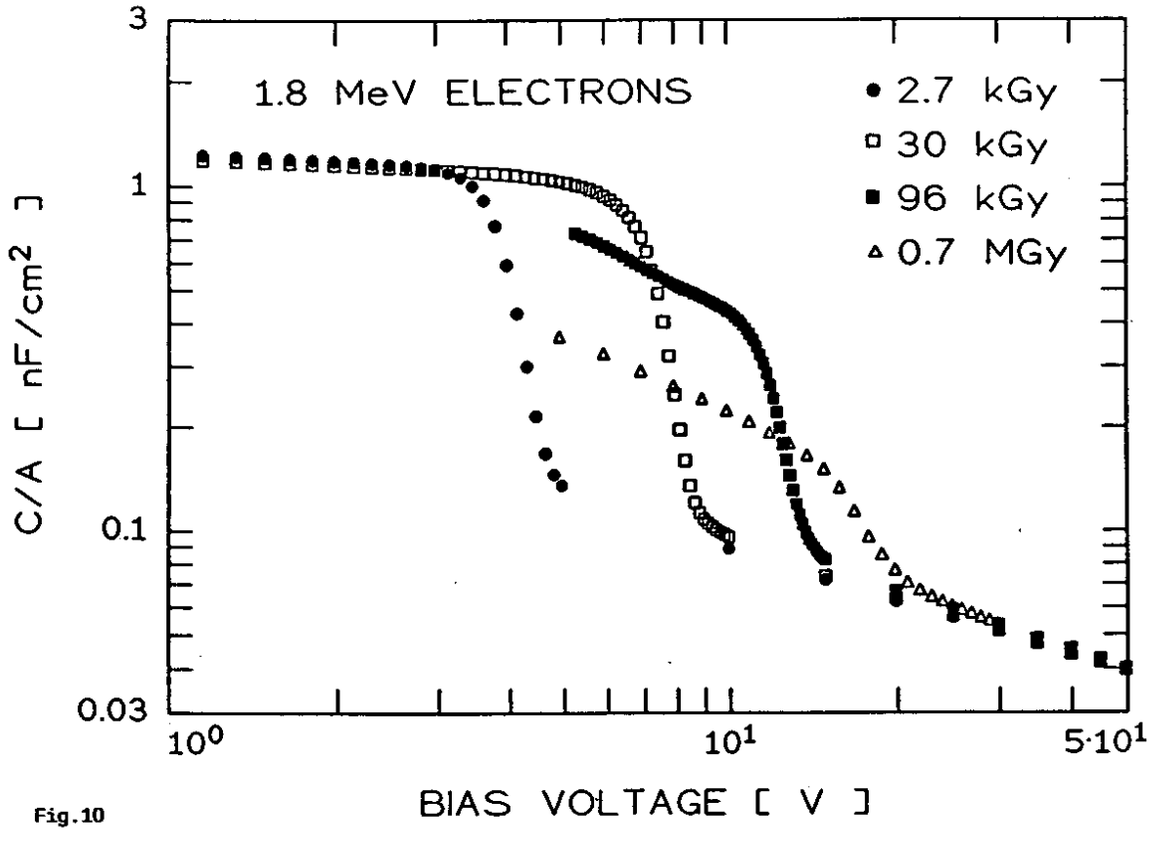
1.8 MeV ELECTRONS
2.7 kGy
30 kGy
96 kGy
0.7 MGy
C/A [ nF/cm$^2$ ]
3
1
0.1
0.03
$10^0$
$10^1$
$5 \cdot 10^1$
BIAS VOLTAGE [ V ]

Fig.10